Moderated Poster Session VI: Basic Science
Friday, October 30, 2015
11:00 a.m. – 12:30 p.m.

P81

Development Of A Sensitive Molecular Imaging System Based On The Transcriptional Activity Of The Peg3 Gene (progression Elevated Gene-3) To Image Castration-resistant Prostate Cancer Cells.

Pallavi Jain, Bertrand Neveu, Yves Fradet, Frederic Pouliot.
University Laval, Quebec, QC, Canada.

Background: Molecular imaging plays an important role in oncology. Unfortunately, the sensitivity of current clinical techniques remains low. New sensitive imaging systems based on cancer specific gene alterations have been developed in the last years. One of them, the Two-Step-Transcriptional Amplification (TSTA) system, can image prostate cancer (PCa) cell gene expression by Positron Emission Tomography (PET) by amplifying PSA promoter activity by 400-fold to generate high levels of reporter expression. Even though the signal achieved by PSA-TSTA is high enough to be detected by clinical PET apparatus in large immune-competent mammals, it is not cancer specific and its activity is mainly driven by androgens. We have studied the potential of the PEG3 (progression elevated gene-3) promoter, a gene highly expressed in cancer cells, to achieve androgen-independent PCa cell imaging.

Methods: Various adenovirus constructs incorporating the PEG3 promoter driving the Firefly luciferase (fl) gene directly, the TSTA system or a newly designed transcriptional amplification system, the 3STA, were generated. The luciferase activities of PEG3-fl, PEG3-TSTA-fl, PEG3-3STA-fl and/or PSEBC-TSTA-fl (Prostate Specific Antigen promoter) were compared by bioluminescence imaging in vitro or in vivo in xenograft mouse models.

Results: The PEG3 promoter driven systems did show very high level of activity in every PCa cell line tested (22Rv1, LAPC4, LNCaP, DU-145, PC-3). Its activity, when incorporated in the amplification systems TSTA and 3STA, was amplified by 11.85 and 49.37 times, respectively, when compared to the activity of the PEG3 promoter alone. In vivo, PEG3-3STA-fl showed 2.2-times higher activity than PSEBC-TSTA that can detect lymph nodes metastasis by PET. Contrary to the PSEBC-TSTA-fl system, the activity of PEG3-3STA-fl was not regulated by androgens and was AR-independent with strong expression observed in castration resistant prostate cancer (CRPC)cells such as DU-145 and PC3.

Conclusions: The above described new imaging system, PEG3-3STA-fl, allows sensitive imaging of AR positive or negative PCa cells. This new amplification system, 3STA allows the PEG3 promoter to produce reporter signal high enough to be detected by PET, a technology available in the clinic. Therefore, this system could potentially image CRPC metastasis with high accuracy in the clinics.

P82

Gene Expression Profiling Distinguishes Stromal Phenotypes Associated With Gleason 3 Versus Gleason 4 Prostate Cancers

Ilinca Georgescu[1], **R. Christopher Doiron**[1], Victoria Tolls[1], J. Robert Gooding[1], Andrew Day[2], D. Robert Siemens[1], Paul C. Park[1].
[1]Queen's University, Kingston, ON, Canada, [2]NCIC Clinical Trials Group, Kingston, ON, Canada.

Background: Much work has been directed at improving the sensitivity of standard prostate biopsy techniques. Considering findings in the tumour microenvironment is other cancers, we hypothesized that the tumour-adjacent stroma in prostate cancer would develop distinct phenotypes in response to G3 versus G4 cancers. This could be used to increase the sensitivity of prostate biopsies by increasing the 'diagnostic reach' of biopsy cores.

Methods: A targeted panel of 107 genes associated with field cancerization was identified using an in silico approach. A discovery cohort of 40 radical prostatectomy samples of Gleason 3+3 and ≥3+4, was identified. mRNA was extracted from laser capture micro-dissected stromal regions adjacent to tumor foci and subjected to targeted gene expression analysis using Nanostring nCounter technology. Post-normalization, univariate and multivariate analyses were used to determine differential expression of genes.

Results: Of 107 identified genes, 9 were significantly differentially expressed between G3 and G4 stroma. Genes, p-values, log2 fold changes (FC) and ROC-AUC values for G4 vs G3 samples are listed as follows: COL1A2 ($p<0.001$, FC=1.92, AUC=0.84) COL1A1 (p=0.010, FC=1.31, AUC=0.81), ACTA2 (p=0.010, FC = 0.95, AUC=0.76) SPARC (p=0.010, FC=1.89, AUC=0.78), LDHB (p=0.015, FC=1.14, AUC=0.74), TIMP1 (p=0.030, FC=1.17, AUC=0.74), CAT (p=0.038, FC = 1.50, AUC=0.76), IGF2 (p=0.039, FC=2.58, AUC=0.82) and SPARC (p=0.009, FC=1.92, AUC=0.71).

Subsequent multivariate pathway analysis revealed two biologically relevant pathways: aerobic glycolysis (PFKFB3, PGK1, PGM1, GLUT1, ACLY, PKM2, LDHA, LDHB, HK2, HMGCS2, ALDOA, ENO1, GAPDH, GLUT3, CMYC, FOXO1, FOXO3) and ECM remodelling (ACTA2, TNC, VIM, TIMP1, SPARC, MMP2, GSN, CNN2, COL1A2, COL1A1), both predictive of G3 and G4 respectively. These pathways suggest an association between a more active metabolic phenotype (p=0.0153, AUC=0.74) and G3, and a more pro-invasion stromal phenotype (p=0.0047, AUC=0.82) and G4. Stepwise logistical regression was then used to identify a subset of these genes (COL1A2, IGF2, NRF2, SPARC, TIMP1), whose average expression was capable of distinguishing G4 from G3 with the greatest predictive power (p=0.008, AUC=0.86).

Conclusions: Stromal cells develop distinct phenotypes in response to G3 versus G4 prostate cancers. Analyses reveal 9 genes and one multivariate model that may be useful in predicting the presence of G4 prostate cancer in a biopsy specimen. These specific gene signatures could be used to increase the 'diagnostic reach' of current prostate biopsy sampling.

P83

On The Way To The Optimization Of The Bladder Tissue Engineering

Sara Bouhout, Stéphane Chabaud, Francine Goulet, **Stéphane Bolduc**.
Laval University, Quebec, QC, Canada.

Background: Despite high morbidity, enterocystoplasty is the gold standard to perform bladder reconstruction surgery, then alternatives were being searched. One among them is tissue engineering. Several scaffolds from synthetic or biological origin have been tested but without been able to support normal bladder urothelial cells (BUC) differentiation, especially uroplakin (UP) plaques and tight junction organization, two essential components of the bladder barrier function. The aim of this study is to define the best combination of scaffold and cells to allow right differentiation of BUC.

Methods: We compared pig native tissue to bladder mucosa equivalent (BME) produced by the self-assembly technique using porcine mesenchymal cells from skin (dFb) or bladder (BMC) biopsies to form the stroma (SA-DFB-BME and SA-BMC-BME respectively) or collagen gel seeded or not with pig BMC (CG-BMC-BME or CG-ACE-BME respectively). SA-derived tissues consisted in cultivating stromal cells in the presence of ascorbate (50µg/ml) for 4 weeks before seeding BUC. CG-derived tissues consisted in

pouring a highly-purified collagen gel (2 mg/ml) before seeding of BUC. After epithelialization, constructs were matured using a culture medium containing retinoic acid (5 x 10-8M) and maintained at the air/liquid interface or immerged in the presence of absence of a urine transitory stimulation (20 min) during medium exchange. Urothelial differentiation was analyzed by hematoxylin/eosin or Masson's trichrome histologies, immunofluorescences (K14, UP), Western blots (pERK/ERK) and electronic microscopy (UP, tight junctions).
Results: SA-DFB-BME allowed uroepithelium stratification but presented high K14 and pERK/ERK levels and immature UP coverage. The use of dFb seemed to switch the urothelial differentiation to a more epidermal one. These negative points were improved in SA-BMC-BME but UP maturation and tight junction organization remained at an unsatisfactory stage. CG-ACE-BME presented a limited proliferation and differentiation of the BUC, clearly highlighting the lack of adequate mesenchymal signals to form a urothelium. Finally, CG-BMC-BME gave impressive results with mature UP plaques and well organized tight junctions especially in the conditions where the tissues remain submerged and were urine-stimulated during maturation.
Conclusions: Ranking the combinations: SA-DFB-BME < CG-ACE-BME < SA-BMC-BME < CG-BMC-BME. In order to produce a near native bladder mucosa equivalent by tissue engineering, the use of organ specific matrix as a scaffold is not mandatory but the use of organ specific mesenchymal cells is an essential requirement combined to a physiological environment (immerged tissue and urine exposition).

P84
Hypoxia And Tissue Engineering In Urology
Stéphane Chabaud[1], Clément Baratange[2], Brice Boiroux[2], Alexandre Rousseau[1], Sara Bouhout[1], Stéphane Bolduc[1].
[1]Laval University, Quebec, QC, Canada, [2]Institut Universitaire de Technologie de Laval, Laval, France.
Background: Tissue Engineering could become an alternative to circumvent the lack of tissues and organs for reconstructive surgeries especially in urology. Nevertheless, these techniques require in-vitro epithelial cells expansion but limited growth or lifespan of the extracted cells or their early and inadequate differentiation often results of the standard cell culture conditions. Also, the air/liquid interface used to start the stratification and maturation of the uroepithelium is a non-physiological condition and results in a hyperproliferation of urothelial cells. In this study, the potential of cell culture in hypoxia was tested during three steps of the urologic tissue reconstruction: the expansion of urothelial cells, the production of the stroma and the maturation of the bladder epithelium.
Methods: 1. Bladder mucosa substitutes were reconstructed using the self-assembly method. Fibroblasts were cultivated in the presence of ascorbate for 4 weeks to produce sheets which were surimposed to form a tridimensional stroma. These stroma were seeded with urothelial cells expanded previously in normoxia or hypoxia and then cultivated in normoxia for 3 weeks at the air/liquid interface. 2. Stroma were produced in normoxia or hypoxia to test the impact of the oxygen reduction on the extracellular matrix formation. 3. Maturation of urothelium on bladder mucosa substitutes was also compared in normoxic or hypoxic conditions.
In 1 and 3, histologic aspect was examined after Masson's trichrome staining. Presence and localization of keratine-14, Ki-67, ZonulaOccludens-1 and Claudin-4 were evaluated by immunofluoresence. Finally, Barrier function was assessed by permeation tests. In 2, Western Blots against collagen type-I and whole Matrix Metallo-Proteinase (MMP) activity measurements were realized.
Results: 1. Hypoxia allowed expansion of usable urothelial cells until passage P7 whereas normoxic conditions limited the use of urothelial cells to passage P4. 2. More collagen type-I was deposited by fibroblasts and less MMP activity was detected in hypoxic cell culture conditions compared to the normoxic ones. 3. A better organization of the urothelial cells basal layer was obtained in hypoxia despite a thinner intermediate layer.
Conclusions: Cell culture in hypoxia could be beneficial to produce engineered urologic tissue: it allowed a longer expansion of epithelial cells and then a reduction in the size of the biopsy, it induced a shorter time of production of the stromal compartment of the engineered tissue, and finally, even if further investigations are needed, it clearly improved urothelial differentiation.

P85
Pudendal but not Tibial Neuromodulation Inhibits Efferent Output from Pontine Micturition Center in Cats
Timothy D. Lyon[1], Brian T. Kadow[1], Zhaocun Zhang[2], Bing Shen[1], Jicheng Wang[1], Audry Kang[3], Andy Lee[3], James R. Roppolo[4], William C. de Groat[4], Changfeng Tai[1].
[1]Department of Urology, University of Pittsburgh, Pittsburgh, PA, USA, [2]Department of Urology, Qilu Hospital, Shandong University, Jinan, China, [3]University of Pittsburgh School of Medicine, Pittsburgh, PA, USA, [4]Department of Pharmacology and Chemical Biology, University of Pittsburgh, Pittsburgh, PA, USA.
Background: Neuromodulation is an FDA-approved treatment for overactive bladder (OAB). Currently the mechanisms underlying neuromodulation are not completely understood. Previous work in cats has suggested that pudendal nerve stimulation (PNS) and tibial nerve stimulation (TNS) can alter afferent sensory signaling from the bladder but the effects on efferent signaling are not known. This study examined the role of PNS and TNS in inhibiting efferent output from the pontine micturition center (PMC).
Methods: Following decerebration in α-chloralose anesthetized cats (n=12), electrical stimulation of the PMC (40 Hz and 0.2 ms for 10-25 seconds) reliably induced bladder contractions of >20 cm H2O with the bladder 60-70% full. PNS (5Hz, 0.2 ms) at two and four times the threshold (2T & 4T) to induce anal twitch was applied to inhibit the PMC stimulation-induced bladder contractions. TNS (5Hz, 0.2 ms) at two and four times the threshold (2T & 4T) to induce toe movement was also studied in the same fashion. Propanolol, a nonselective β-adrenergic antagonist, was administered intravenously (1 mg/kg) to a subset of cats (n=5) to determine the role of β receptors in PNS/TNS inhibition. Sacral dorsal nerve roots (S1-S3) were transected in a second group of cats (n=4) to determine whether reflex afferent sensory input was affecting PMC output via a feedback mechanism.
Results: PNS at both 2T and 4T significantly ($p<0.05$) inhibited the amplitude and area under the curve of the bladder contractions induced by PMC stimulation. TNS did not significantly inhibit bladder contractions induced by PMC stimulation. Propanolol removed the PNS inhibition. Dorsal root transection did not significantly alter bladder response to PMC stimulation suggesting that reflex afferent signaling was not influencing the results.
Conclusions: This study reveals that PNS but not TNS inhibits the efferent arc of the spinobulbospinal micturition reflex via β-adrenergic signaling in cats. It is likely that the β-adrenergic input is delivered via the hypogastric nerve. Developing a clearer understanding of the neuroanatomic and pharmacologic pathways involved in neuromodulation could provide targets for novel OAB therapies.

P86
A PCA3 Gene-Based Transcriptional Amplification System Targeting Primary and Metastatic Prostate Cancer Cells
Pallavi Jain, Bertrand Neveu, Yves Fradet, Frédéric Pouliot.
University Laval, Quebec, QC, Canada.
Background: PCA3 non-coding long RNA is a unique prostate cancer (PCa) biomarker that has been widely studied for its sixty-fold overexpression in PCa cells, compared to benign prostate cells. While this gene has been exploited as an accurate diagnostic urine biomarker for PCa detection, other clinical applications have yet to be seen. In this study, the proximal PCA3 promoter was introduced into a new transcriptional amplification system named the 3-Step Transcriptional Amplification System (PCA3-3STA).
Methods: This system was cloned into a type 5 adenovirus and was tested for its specificity to image PCa cells by bioluminescence quantification and in vivo imaging.

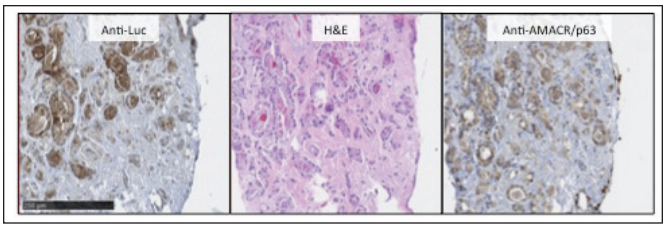

Fig. 1. P86.

Results: PCA3-3STA activity was highly specific for PCa cells, ranging between 98.7 and 108.0-fold higher, respectively, than that for benign prostate or non-PCa cells. In PCa cell line mouse xenografts, PCA3-3STA was shown to image PCA3 promoter activity with high sensitivity. Moreover, when primary PCa biopsies were infected with PCA3-3STA, it managed to image PCa epithelial cells but not stromal cells (Fig. 1).
Conclusions: PCA3-3STA therefore represents a prostate- and PCa-specific expression system with the potential to target, with high accuracy, PCa epithelial cells for imaging, vaccines, or gene therapy.

P87
Combined Inhibition Of Wee1 Kinase And Heat Shock Protein-90 In The Treatment Of Urothelial Cancer

Mahmoud Chehab, Richard Cotran, Diana Dunn, Alosh Madala, Mark Woodford, Sami Jamal, Gennady Bratslavsky, Mehdi Mollapour, Dimitra Bourboulia.
Upstate Medical University, Syracuse, NY, USA.

Background: Heat Shock Protein 90 (Hsp90) is an essential molecular chaperone in eukaryotes and is critical for the stability and activity of numerous cellular client proteins involved is signaling pathways in both normal and tumor cells. Inhibition of Hsp90 has the potential to cripple the tumorigenic and metastatic potential of cancer cells. Our previous work has shown that Wee1 kinase is an Hsp90 client and it directly phosphorylates and regulates the chaperone activity of Hsp90. Pharmacologic inhibition of Wee1 sensitizes tumor cells to chemotherapeutic agents. Our previous work has also shown that combination of Hsp90 and Wee1 inhibitors (Wee1i) promote apoptosis in prostate cancer. Here we evaluated the efficacy of the new generation of Hsp90 inhibitor Ganetespib in combination with a Wee1i in urothelial cancer cells (UCC). We first determined the cellular uptake of the fluorescent Ganetespib by UCC in combination with Wee1i. We next demonstrated binding of intracellular Hsp90 protein to biotinylated Ganetespib in UCC pre-treated with Wee1i. Finally, we evaluated the effects of Wee1i and Hsp90 inhibition on UCC proliferation, cell cycle, and apoptosis.
Methods: We used four established UCC lines (T24, RT4, J82, UMUC3) as models for invasive and noninvasive UC. SVHUC cell line was used as a model for normal urothelial cells. We identified optimal concentrations of Wee1i and Ganetespib for each cell line that caused minimal cell death/apoptosis. Cell lines where then treated with each drug alone or in combination. Flow cytometry was used to analyze drug uptake and effects on cell cycle; western blots were used to evaluate drug binding; trypan blue was used to evaluate cell viability and MTT assay was used to evaluate proliferation.
Results: Wee1i increases the uptake of fluorescent Ganetespib by advanced UCC but not early stage UCC leading to an increase in response to combination treatment. The combination of Wee1i and Ganetespib causes increase in apoptosis and decrease of tumor cell proliferation. The inhibition of Wee1 effectively abrogates the Ganetespib-induced G2/M arrest in UCC, forcing the cells into premature catastrophic mitosis, thus enhancing cell death after treatment with Ganetespib.
Conclusions: In advanced UCCs, we show that pharmacologic inhibition of Wee1 kinase sensitizes UCC to Hsp90 inhibitor. Our data suggest that combined targeting of Wee1 and Hsp90 could potentially become a novel therapeutic strategy in patients with advanced urothelial cancer.

P88
3-D In Vitro Urothelium Infection Model Using The Self-assembly Technique

Hazem Orabi[1], **Vitalie Railean**[2], Stephane Chabaud[2], Stéphane Bolduc[1].
[1]Urology Department, Université Laval, Quebec, QC, Canada, [2]LOEX, Université Laval, Quebec, QC, Canada.

Background: Previous in vitro and in vivo studies for investigating the development and differentiation of the urothelium have been limited, as they do not represent the normal urothelial development and differentiation process in human. Self-assembly method of matrix formation would form a biomimetic tissue without the need for exogenous materials. In this study, we aimed at the creation of an ex-vivo urinary bladder model and investigating post-infection effects on the urothelium and changes in the cytokeratin expression.
Methods: Bladder stromal (BSCs), urothelial (UCs), and smooth muscle cells (SMCs) were isolated using enzymatic methods. BSCs were stimulated with ascorbate to form collagen sheets. Following, SMCs and UCs were sequentially seeded on the stacked BSC-sheets to form bladder equivalents. After maturation, constructs were analyzed by histology, mechanical tests and permeability studies. Then, the ex vivo bladder model was subjected to epithelial bacterial infection. Effects on urothelial proliferation and keratin expression were noted.
Results: BSCs formed collagen sheets that could be handled easily. UCs constituted a well-differentiated epithelial layer with biomarkers of impermeability. A well-formed basement membrane and SMCs bundles were identified. Post-infection effects included decrease in constructs` thickness, urothelial hyperplasia, increased expression of CK14 and loss of CK20 expression, reflecting skin phenotype changes
Conclusions: Using the self-assembly, in vitro bladder model was created with many functional and biological similarities to native bladder tissue without any foreign material. The post-infection changes represent a normal urothelial response to injury, which if not reversed, may lead to squamous metaplasia of the urothelium.

P89
Role of Fibroblast Growth Factor Receptors in Leydig Cell Development

Andres F. Correa[1], Kenneth Walker[2], Daniel Bushnell[2], Caitlin Schaefer[2], Julia Schaefer[2], Carlton Bates[2].
[1]University of Pittsburgh, Pittsburgh, PA, USA, [2]University of Pittsburgh Childrens Hospital, Pittsburgh, PA, USA.

Background: The adult Leydig cell undergoes several stages of maturation during development which is closely regulated by luteinizing hormone (LH), thyroid hormone (TH) and androgens. Several studies have shown increased androgen production byLeydig cells when exposed to fibroblast growth factors (Fgfs). The role of Fgf signaling in Leydig cell development and function remains unknown.
Our aims are to investigate 1) Leydig cell development and maturation using a lineage tracing marker 2) the effect fibroblast growth factor receptor 1 and 2 (Fgfr1/2) deletion on adult Leydig cell development and function.
Methods: Tbx18cre transgenic mice, which express cre in Leydig cells, were bred to either a CAG/red fluorescent protein (RFP) reporter (for lineage tracing) or to Fgfr1 and Fgfr2 floxed mice (for conditional knockouts of the receptors). Immunohistochemisty assays were performed to assess the expression pattern of the Tbx18creCAG line in the testis. Sox9 and 3-βHSD were used as markers of Sertoli cells and Leydig cells respectively. Leydig cell development in the Fgfr knock-out model was determined by gene expression using Real Time PCR at day 1, 30, 45 and 60 post birth. Leydig cell maturity was assessed with the following gene library: fetal Leydig cell (Patched and Thsb 2), immature (5-α-reductase) and mature (Cyp17a1, Ptgds, Sult1e1, and Hsd17b3).
Results: Immunohistochemical analysis of the Tbx18creCAG mice revealed RFP expression throughout testicular interstitial cells of both fetal and adult testis. Immunolabeling with 3-βHSD and Sox9 revealed co-labeling of the RFP and 3-βHSD, but not with Sox9, indicating that Tbx18cre gene expression was only in the Leydig cell. RFP-labeled Leydig cell numbers appeared to similar from embryonic stages through postna-

tal life, including no apoptosis at any stage. Tbx18creFgfr1/2 knock-out mice showed under-developed Wolffian duct-derived structures in post-pubertal mice compared to controls. Fetal Leydig cell gene expression markers between controls and the Fgfr1/2 knockouts were comparable from birth to maturity. Adult mutant mouse testicles did have increased expression of 5-α-reductase and decrease expression of Cyp17a1, Ptgds, and Sult1e1 consistent with lack of leydig cell maturation.
Conclusions: Tbx18cre mice express cre only in Leydig cells, starting in embryos, making it an ideal to lineage trace or manipulate gene expression in Leydig cells. Tbx18creFgfr1/2 knockout mice had increased expression of immature Leydig cell gene markers compared to controls, consistent with Leydig cell arresting in an immature state. Thus, Fgfr1 and 2 signaling appears to be critical for Leydig cell maturation from an immature to a mature state. Impaired Fgf signaling in the Leydig cell may be responsible for some forms idiopathic hypogonadism.

P90

MicroRNAs as Potential Biomarkers to Predict Risk of Urinary Retention Following Intradetrusor onabotulinumtoxin-A Injection

Brian Kadow, Christopher Chermansky, Mahendra Kashyap, Subrata Pore, Pradeep Tyagi.
University of Pittsburgh Medical Center, Pittsburgh, PA, USA.

Background: Recent research has highlighted the role of microRNAs (miRs) in the progression of chronic diseases, which represent a new level of epigenetic post-transcriptional control of gene expression. However, their role in overactive bladder (OAB) and underactive bladder (UAB) is unknown. We studied miR expression in OAB patients injected with intradetrusor onabotulinumtoxin-A (BoNT-A) and we compared patients who developed elevated post-void residual volumes after treatment (PVRs >200mL) to those who maintained normal PVRs.
Methods: 9 female OAB patients aged 45-80 (Mean 66.2) with urge urinary incontinence (UUI) or urge-predominant mixed urinary incontinence (MUI) refractory to at least two anticholinergic medications were consented for this IRB-approved study. Cystoscopic-guided punch bladder biopsy was obtained at the time of injection of 100U BoNT-A. Total RNA isolated from biopsy tissue was converted to cDNA so as to assess the differential expression of 13 different miR species, chosen because of their known effect on neurotrophin expression and smooth muscle function. Quantitative real time reverse transcription-polymerase chain reaction (qRT-PCR) was performed on the cDNA obtained from each patient in triplicate, and relative levels of expression for selected miR species were normalized to the expression of U6 small nuclear endogenous gene. PVRs were measured by ultrasound at the three week follow-up visit (Fig. 1).
Results: 5 patients had PVRs <200mL (Range 0 – 88mL, Mean 40mL) after BoNT-A treatment, and these patients formed the low PVR group. The other 4 patients had PVRs >200mL (Range 213 – 518mL, Mean 321mL) after BoNT-A treatment, and these patients formed the high PVR group. There was no age difference between the two groups (p = 0.85). We noted differential expression of 5 miRs between the two groups, specifically miR26a/b, miR125b, miR210 and miR221. The high PVR group showed a 5-fold upregulation of miR26a/b and a 2-fold downregulation of miR210, miR125b, and miR221.
Conclusions: miR-210 is considered a neuroprotective mediator against ischemia, and its relatively higher expression was associated with normal PVR after BoNT-A injection. Other groups have shown that the upregulation of miR26a is associated with smooth muscle stretching, and increased miR26a expression could predispose OAB patients to an increased risk of urinary retention after BoNT-A. This study suggests that determining miR expression prior to BoNT-A treatment in OAB patients might help to determine which patients are at risk of developing elevated PVRs following therapy.

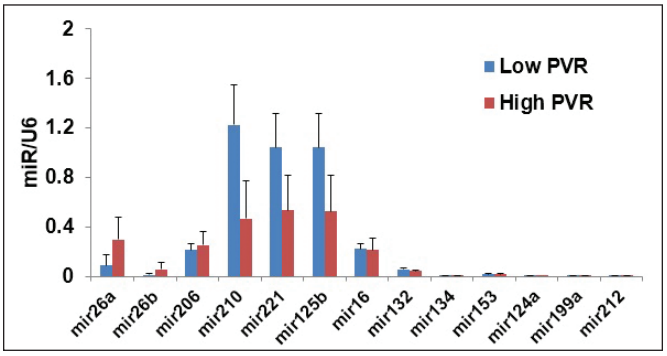

Fig. 1. P90.

P91

Hydrogen Sulfide Ameliorates Renal Injury Associated With Chronic Obstructive Uropathy

Shouzhe Lin[1], Fazil Visram[2], Ian Lobb[1], Amy Mok[3], Jifu Jiang[3], Matthew Whiteman[4], Weihua Liu[5], Aaron Haig[5], Alp Sener[3].
[1]Department of Microbiology and Immunology, Western University, London, ON, Canada, [2]Department of Physiology and Pharmacology, Western University, London, ON, Canada, [3]Matthew Mailing Centre for Translational Transplant Studies, London Health Sciences Centre, London, ON, Canada, [4]The University of Exeter, Exeter, United Kingdom, [5]Department of Pathology, Western University, London, ON, Canada.

Background: Obstructive uropathy is characterized by blockages in the urinary tract. Prolonged obstruction can cause fibrosis, leading to irreversible renal injury and chronic kidney disease (CKD). Patient prognosis is heavily dependent on the level of renal injury. Although there are surgical and non-surgical treatments available to remove obstructions, preemptive measures aimed at mitigating renal injury during obstruction are limited. Hydrogen sulphide (H2S) is an endogenous gasotransmitter that mediates physiological processes such as cellular signaling and vasodilation. Recent studies have shown that H2S can mitigate renal injury associated with acute obstruction via multiple anti-apoptotic, anti-inflammatory and anti-oxidant properties. The current study investigates the protective role of exogenous H2S treatment against chronic obstructive uropathy.
Methods: Male Lewis rats underwent complete unilateral ureteral obstruction (UUO) via ligation of left ureter with silk sutures. Following UUO, animals were given daily injections of either phosphate buffered saline (PBS) or 200 μM/kg GYY 4137 (slow-releasing H2S donor) + PBS for 30 days. Urine and serum samples were collected on post-operative days 3, 10, 20 and 30 to monitor parameters of renal function and injury. Kidneys were removed on day 30 for histological analysis. Sections were stained with Hematoxylin & Eosin (H&E), Terminal deoxynucleotidyl transferase dUTP nick end labeling (TUNEL) and Masson s trichrome stain to assess renal cortical thickness, apoptosis and fibrosis, respectively. Additionally, sections were immunohistochemically stained with antibody against myeloperoxidase (MPO) to assess neutrophil infiltration.
Results: H2S treated animals exhibited significantly greater ($P<0.05$) retention of renal cortical thickness and markedly reduced proteinuria during chronic renal obstruction compared to PBS treated animals. In addition, H2S treatment significantly ameliorated renal fibrosis ($P<0.01$) following chronic obstruction when compared to PBS treatment. H2S treatment also decreased renal apoptosis and neutrophil infiltration in chronically obstructed kidneys compared to PBS treatment.
Conclusions: Our findings suggest that supplemental H2S can mitigate renal injury associated with chronic obstruction. H2S may represent a cost-effective preemptive therapy against renal damage associated with chronic obstructive uropathy, potentially improving long-term renal function following resolution of renal obstruction.